

Assimilation of radar observations of a supercell storm using 4DVar: Parameter retrieval experiments.

N. Andrew Crook¹, David Dowell², Juanzhen Sun¹ and Ying Zhang¹

1. National Center for Atmospheric Research*, Boulder, Colorado

2. Cooperative Institute for Mesoscale Meteorological Studies, Norman, Oklahoma

1. INTRODUCTION

As the horizontal gridspacing of Numerical Weather Prediction (NWP) models decreases into the sub-10 km range, the potential to explicitly resolve and numerically forecast convective storms becomes a reality. The primary method for observing these storms is with radar. Hence, to initialize a storm in an NWP model requires the assimilation of radar data. The incorporation of convective storm data into NWP models represents a large departure from traditional NWP. Previously, these small scale storms were considered “noise” which needed to be filtered out of the initial conditions. For example, if a radiosonde ascended in a convective storm, the observed sounding would be considered unrepresentative of the mean flow and every effort would be made to filter out such observations. Hence, incorporating storm data into NWP models requires a new approach to data assimilation.

A number of methods for assimilating radar data into numerical models have recently been proposed and tested. Among these are nudging, 3D Variational data assimilation (3DVar), the Ensemble Kalman Filter (EnKF) and 4D Variational data assimilation (4DVar). In this study, we test the performance of 4DVar in retrieving the structure of an observed convective storm. We will also test the ability of 4DVar to retrieve some of the parameters in the underlying cloud model.

The case we have chosen for this study is the 17 May 1981 Arcadia, OK, supercell that was observed by two Doppler radars (at Cimarron and Norman) spaced approximately 40 km apart. (This storm was the subject of a single Doppler retrieval study by Weygandt et al. (2002) and an EnKF retrieval study by Dowell et al. (2004)) In this study we assimilate data from the Cimarron radar and compare the results with dual-Doppler analyses.

* The National Center for Atmospheric Research is sponsored by the National Science Foundation.

Corresponding author address: Andrew Crook, NCAR, P.O. Box 3000, Boulder, CO 80307-3000; crook@ucar.edu

2. 4DVAR TECHNIQUE

The objective of the 4DVar technique is to find an initial state that upon model integration produces output fields that fit the observations as well as a background field as closely as possible. The background field is typically valid at the initial time, whereas the observations can be spaced at any time throughout a specified time window. A cost function, measuring the misfit between the model forecast and both the background field and observations of radial velocity, v_r^{obs} and rainwater (converted from reflectivity) q_r^{obs} , is defined. Assuming that the observational errors are uncorrelated in space and time, the cost function, J is given by

$$J = \sum_{\sigma, \tau} \eta_v (v_r - v_r^{obs})^2 + \eta_{q_r} (q_r - q_r^{obs})^2 + J_b + J_p \quad (1.1)$$

where σ represents the spatial domain and τ represents the temporal domain. The quantities η_v and η_{q_r} are weighting coefficients that represent the inverse of the observational error (squared) of the radial velocity and rainwater data, respectively. The model radial velocity v_r is calculated from the Cartesian velocity components (u, v, w) through:

$$v_r = u \frac{x - x_r}{r} + v \frac{y - y_r}{r} + (w - w_i) \frac{z - z_r}{r} \quad (1.2)$$

where w_i is the fallspeed of precipitation.

The term J_b in (1.1) represents the fit to the background field. In this study, the background field is given by the previous analysis, if it exists, or by a large-scale sounding in the absence of a previous analysis. The term J_p represents a penalty term that seeks to minimize excessive temporal and spatial variations.

The numerical model that is used in the 4DVar technique is an anelastic, nonhydrostatic,

storm-scale model (Sun and Crook, 1997). The prognostic variables include the three velocity components, the perturbation liquid-water potential temperature, rainwater mixing ratio, and total water mixing ratio. The horizontal/vertical gridspacing of the model is 2 km/500m

3. DATA

For a detailed description of the Arcadia, OK dataset the reader is referred to Dowell and Bluestein (1997). Briefly, the storm was observed on 17 May 1981 by two Doppler radars (at Cimarron and Norman). The baseline between the two radars is approximately 40 km oriented in a NW-SE direction (Cimarron in the northwest). The reflectivity and radial velocity observations from both radars were interpolated in the horizontal to a Cartesian grid with a horizontal grid spacing of 2 km using a Cressman scheme. In the vertical, the data were left on their original constant elevation surfaces. In this study, only the first two radar volumes are assimilated, at $t = 1630, 1634$ CST.

The dual Doppler analysis was obtained by objectively analyzing the Norman and Cimarron data onto a Cartesian grid (same as the model grid) using a Cressman scheme with a radius of influence of 2000 m in the horizontal and 1000 m in the vertical. The wind field was synthesized with an iterative method that satisfies $w=0$ at the ground and storm top.

The sounding that is used to specify the large-scale environment is described in the paper by Dowell et al. (2002).

4. WIND FIELD RETRIEVAL

Fig. 1 shows the retrieved vertical velocity (contours) overlaid on the retrieved horizontal velocity field (vectors) at $z = 2.25$ km. The time shown is 1634 CST, after the assimilation of two volumes of data from the Cimarron radar. For comparison, the velocity fields from the dual Doppler analysis are shown in the lower panel. The dual Doppler analysis shows the presence of two updraft cores; the stronger core to the south has a maximum vertical velocity of 11.3 m/s at 2.25 km. As can be seen the 4DVar analysis captures the southern updraft, with a w_{max} of 9.8 m/s at the same level. However, the northern updraft, which is admittedly a very transient feature in the dual Doppler analyses, is not captured with 4DVar.

The analyses from 4DVar have been compared against independent observations from the second radar at Norman as well as observations from a 444 meter tower that the storm passed over. The comparisons against the Norman observations were presented in Crook and Dowell (2003). Comparisons against the tower data will be shown at the Conference.

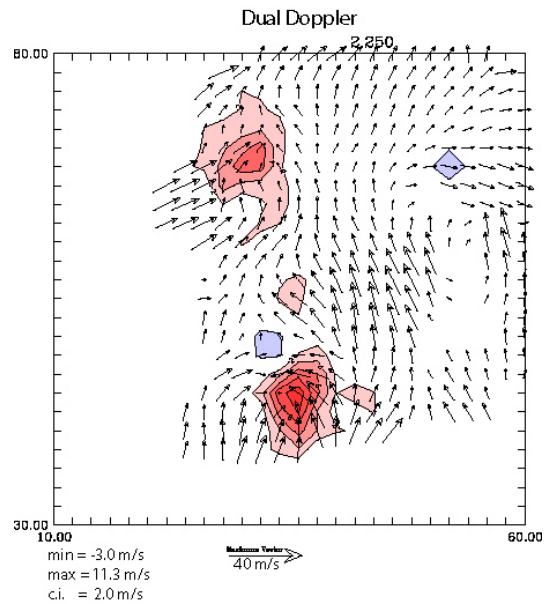
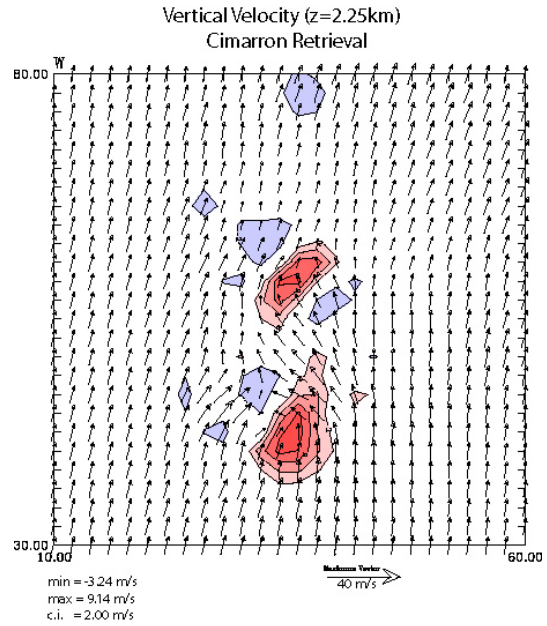


Figure 1. Vertical velocity (contours) overlaid on horizontal velocity vectors at $z = 2.25$ km from 4DVar (top panel), and dual Doppler (lower panel). Time = 1634 CST.

5. PARAMETER RETRIEVAL

One of the strengths of the 4DVar technique is its ability to retrieve not only the initial conditions of the underlying numerical model but also some of the parameters in that model. In this section we report on some early parameter retrieval experiments.

The first step was to test the sensitivity of the retrieved initial fields to a number of model parameters. The parameters examined were the

diffusion coefficient, coefficient in the evaporation equation and the rainwater fallspeed. A series of assimilation experiments were performed with the parameters fixed during the run but varying between experiments. The final cost function (after 100 iterations) as well as the fit to the observations from the second radar was then examined for each experiment. It was found that the retrieved initial fields were relatively insensitive to the diffusion coefficient and evaporation coefficient. However, a strong sensitivity to the fallspeed parameter was found. The fallspeed in the Sun and Crook model is given by:

$$w_t = F \left(\frac{p_o}{p} \right)^{0.4} q_r^{0.125} \quad (1.3)$$

where the parameter $F \equiv F_d = 5.4$ m/s in the control model and q_r has the units of g/kg. Figure 2 shows the sensitivity of the final cost function to the parameter F for five experiments with F/F_d varying between 0 and 2.

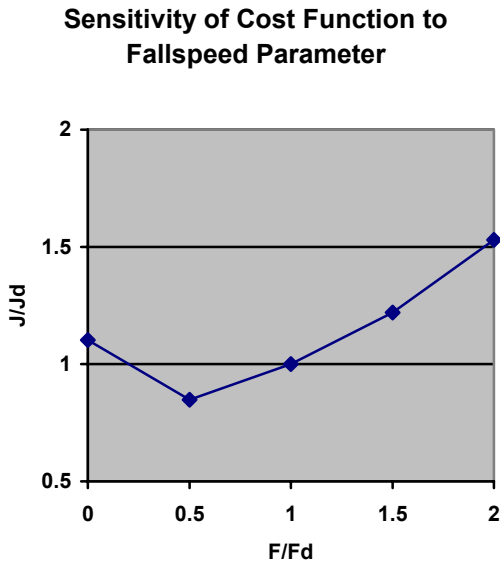


Figure 2. Sensitivity of the final cost function J to the fallspeed parameter F (normalized by F_d). The cost function, J , is normalized by the cost function J_d obtained using the default fallspeed.

Figure 2 shows that the final value of the cost function varies by almost a factor of two as F/F_d varies from 0 to 2, with the lowest value at $F/F_d = 0.5$. This sensitivity suggests that we may be able to retrieve this parameter by making it a control variable.

The method of parameter retrieval follows that described in Zhu and Navon (1999). The parameter F is defined as a control variable

and the gradient of J with respect to F is calculated in the same manner as the initial conditions of the model. We note that there are two contributions of the fallspeed to the cost function; a direct contribution through its effect on the model-calculated radial velocity (1.2) and an indirect contribution through the tendency of the model fields (determined by the equations of motion). At the Conference we will show the relative contributions of both effects.

In addition to making F a control variable, an extra penalty term was added to the cost function to ensure that F remained in a realistic range. The form of this penalty term was taken as:

$$J_p(F) = \begin{cases} \frac{1}{2}(F - 0.5F_d)^2 & \text{if } F < 0.5F_d \\ 0 & \\ \frac{1}{2}(F - 2F_d)^2 & \text{if } F > 2F_d \end{cases} \quad (1.4)$$

This penalty term ensures that F does not stray too far outside of the range of $[0.5F_d, 2F_d]$, however there is no penalty if F remains in that range.

We then ran the same experiment as before, but this time with F as a control variable. The first guess for F was taken as the value in the control model; i.e. $F=5.4$. Figure 3 shows the variation of F with iteration number.

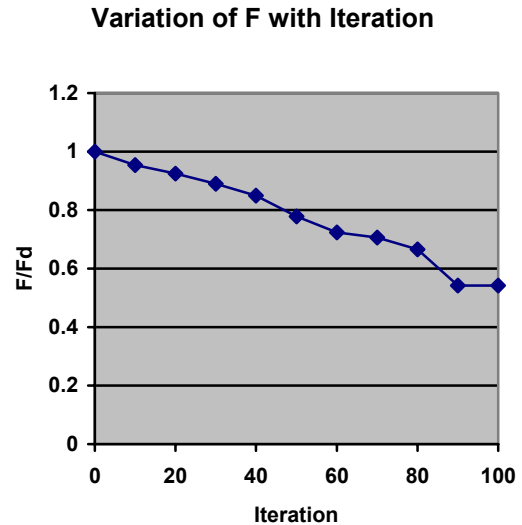


Figure 3. Variation of the fallspeed parameter, F (normalized by the value in the control experiment, F_d) with iteration.

As can be seen, the value of F steadily decreases throughout the experiment, leveling off in the last 10 iterations at a value of $F/F_d = 0.54$.

We note that this is very close to the value of F that gave the minimum cost function in the experiments with fixed F (Fig. 2).

We conclude by showing the effect of using the retrieved fallspeed on short-term forecasts of the Arcadia storm. Figure 4 shows 40 minute forecasts of the storm using the default fallspeed (top panel) and the retrieved fallspeed (lower panel). Shown is the reflectivity field at 0.25 km overlaid on the horizontal velocity field. As can be seen, the position of the storm in the two forecasts is approximately the same. However, the structure of the storms is somewhat different; the storm with the retrieved fallspeed is stretched downshear. Clearly, the lowered fallspeed is allowing precipitation to travel further downwind of the main updraft

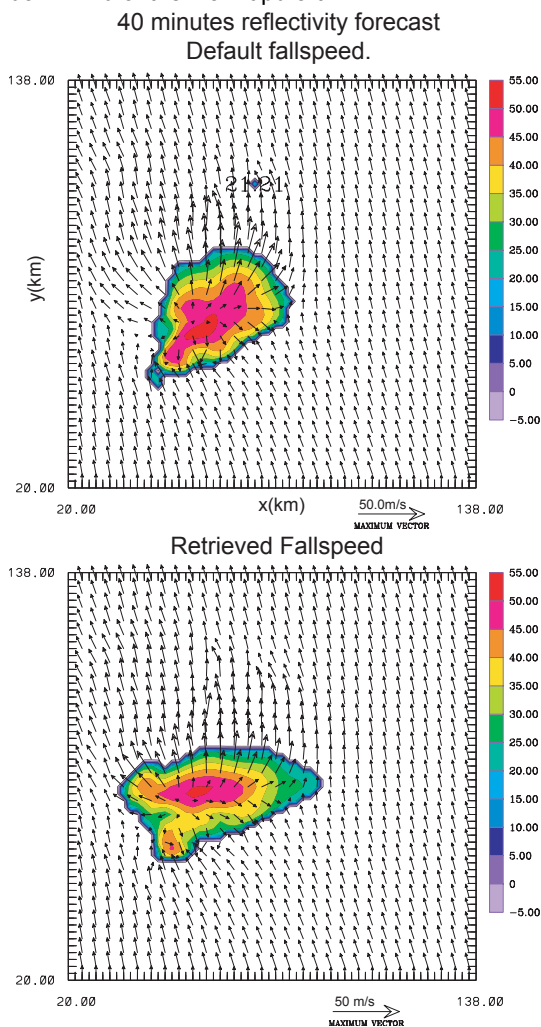


Figure 4. 40 minute forecasts of the Arcadia storm using the default fallspeed (top panel) and the retrieved fallspeed (lower panel). Shown is the reflectivity at $z=0.25$ km overlaid on the horizontal velocity field.

CONCLUSION

We have applied the 4DVar technique to Doppler radar observations of the Arcadia supercell. Experiments have been performed in which data from one Doppler radar are assimilated and then compared with observations from a second radar, dual Doppler analyses and tower data (results to be presented at the Conference). We have also performed some initial experiments to retrieve parameters in the underlying numerical model. It was found that the retrieved initial conditions were most sensitive to the parameter governing the fallspeed in the model. An experiment was performed in which the fallspeed was taken as a control variable and then retrieved by finding the value which minimized the cost function. The retrieved fallspeed was approximately half that used in the control model. Finally, it was then shown that this retrieved fallspeed has a noticeable effect on short term forecasts of the Arcadia supercell, particularly in the structure of the storm.

REFERENCES

- Caya, A., J. Sun and C. Snyder, 2002: A comparison between the 4DVar and Ensemble Kalman Filter techniques for radar data assimilation. 19th Conf. On Weather Analysis and Forecasting, San Antonio, TX, 327-330.
- Crook, N.A. and D. Dowell, 2003: Assimilating radar observations of a supercell storm into a cloudscale model: 4DVar and Ensemble Kalman Filter methods. 31st Conf. On Radar Meteorology, Seattle, WA, 154-157.
- Dowell, D. C., and H.B. Bluestein, 1997: The Arcadia, Oklahoma, storm of 17 May 1981: Analysis of a supercell during tornadogenesis. *Mon. Wea. Rev.*, **125**, 2562-2582.
- Dowell, D. C., F. Zhang, L. Wicker, C. Snyder, B. Skamarock and N.A. Crook, 2002: Wind and temperature retrievals of 17 May 1981 Arcadia, Oklahoma, Supercell: Ensemble Kalman filter results. *Mon. Wea. Rev.*, **132**, 1982-2005.
- Sun, J. and N. A. Crook, 1997: Dynamical and microphysical retrieval from Doppler radar observations using a cloud model and its adjoint. Part I: Model development and simulated data experiments. *J. Atmos. Sci.* **54**, 1642-1661.
- Weygandt S. S., A. Shapiro, K.K. Droegemeier, 2002: Retrieval of Model Initial Fields from Single-Doppler Observations of a Supercell Thunderstorm. Part I: Single-Doppler Velocity Retrieval. *Mon. Wea. Rev.* **130**, 433-453.
- Zhu, Y and I.M. Navon, 1999: Impact of parameter estimation on the performance of the FSU Global Spectral model using its full physics adjoint. *Mon. Wea. Rev.* **127**, 1497-1517.